2020 IEEE/RSJ International Conference on Intelligent Robots and Systems (IROS)
October 25-29, 2020, Las Vegas, NV, USA (Virtual)

Anticipating tumor metastasis by circulating tumor cells captured by acoustic microstreaming

Xue Bai, Bin Song, Dixiao Chen, Yuguo Dai, Lin Feng*, Fumihito Arai

***Abstract*—Circulating tumor cells (CTCs) are the primary cause of tumor metastasis after surgery. Metastatic tumor recurrence is the leading reason of cancer death. It is prerequisite to develop a platform for CTCs separation to predict the cancer cell transfer in important organs. Herein, a novel acoustic microfluidic device was designed to capture the "true" CTCs from the whole blood sample. The blood got from the mice with breast tumors removed. There are some CTCs that have escaped from the solid tumor contained in these blood samples, instead of artificially mixing individual tumor cells into normal blood. In addition, the predictions of tumor prognosis are made based on the number of CTCs captured by the acoustofluidic device. Finally, the prediction has been confirmed through long-term observation of mice with tumor excised. The acoustofluidic device can efficiently capture CTCs and predict the tumor metastasis, which can help clinicians plan follow-up treatment for patients who have had their tumors surgically removed.**

I. INTRODUCTION

Circulating tumor cells (CTCs) are "seeds" and can directly travel through the haematogenous system[1] or sequentially use both the lymphatic and blood vasculature to colonize distant organs[2, 3], which means the formation of tumor metastasis. Metastatic tumor recurrence is the cause of about 90% of cancer-related deaths[4, 5]. Therefore, CTCs has been a novel diagnostic and prognostic biomarkers in therapeutic assessments to provide valuable guidance for cancer therapy[6-9]. However, CTCs are extremely rare (1-3000 CTCs/mL) [10], compare to the high background of 10^9 red blood cells (RBCs) and 10^7 white blood cells (WBCs) per milliliter[11]. In addition, structural, biological, and functional integrity should be retained for the downstream analysis[12].

*Research supported by the Natural Science Foundation of Beijing (No.17L20128) and the National Key R&D Program of China (No. 2019YFB1309702)

Xue Bai is with Beihang University; School of Mechanical Engineering & Automation, Beihang University, Beijing 100083, China, (e-mail: baixue041104@163.com).

Bin Song is with Beihang University; School of Mechanical Engineering & Automation, Beijing, China (e-mail: daiyuguo5612@163.com).

Dixiao Chen is with Beihang University; School of Mechanical Engineering & Automation, Beijing, China (e-mail: liangsz13nq@buaa.edu.cn).

Yuguo Dai is with Beihang University; School of Mechanical Engineering & Automation, Beijing, China (e-mail: daiyuguo5612@163.com).

Lin FENG is with Beihang University; School of Mechanical Engineering & Automation, and also with Beijing Advanced Innovation Center for Biomedical Engineering, Beihang University, Beijing 100083, China, (e-mail: linfeng@buaa.edu.cn).

Fumihito Arai is with the Department of Micro-Nano Mechanical Science & Engineering, Nagoya University, Nagoya 464-0814, Japan (e-mail: arai@mech.nagoya-u.ac.jp).

At present, the separation methods of CTCs can be divided into two categories: antibody dependent or antibody independent [13]. Antibody dependent methods, in general, integrate the tumor-specific antibodies and magnetic or fluorescence markers to isolated CTCs from other blood cells[14, 15]. Because of the expression of certain biomarkers is a highly dynamic and heterogeneous process in different cancer or patient[16]. Even in the same patient, cancer cell biomarker is highly heterogeneous[17, 18]. Therefore, a priori knowledge of relevant antibodies is required before the CTCs separation and the separation efficiency depends heavily on the selection of antibodies[19]. Antibody independent methods is usually based on physical properties, size, deformability, and electrical properties, that are essentially different from those of blood cells[20].

The label-free approaches relied on microfluidic chip stand out from a crowd of methods that suffer from time consuming, extensive blood samples, lost target cells and labor-intensive operation [19, 21]. This method is extremely versatile that are independent of the biomarker' specific expression, and could address the cellular damage caused by contact capture that because of the non-contact operation. This acoustics-fluidic method relies on the steady localized microstreaming forces generated by the vibrating bottom cavity array, which are capable of trapping CTCs[22]. The oscillatory motion is driven by acoustic field, a power intensity and frequency even lower than the ultrasonic imaging in clinical, which has been proven safe on human tissue and cells[19]. Acoustics-fluidic method is more likely to maintain the intrinsic properties of CTCs for further analysis. However, these methods are always applied to isolate the "definite" CTCs from the mixture of cancer cell and health blood[23], not patient blood with "true" CTCs from the solid tumor. This shortcoming severely limits the conversion of this method to clinical application. Some studies have used these methods to separate the " true" CTCs from patient blood[24]. However, the prognostic based on these data and the formation of metastasis cannot be confirmed.

Herein, an integrates acoustics and microfluidics are presented to efficiently and stably capture the CTCs from whole blood sample from mice whose tumors had been surgically removed for anticipating tumor metastasis and follow-up verification in the same mice. This acoustics-microfluidics approach can be simple-to-fabricated and easy-to-operate. The mouse model in this study completely simulated the whole process of tumor formation, surgical resection and postoperative recovery in clinical practice, which can systematically evaluate the effectiveness of the acoustofluidic device for CTCs separation.

II. METHODS AND MATERIALS

A. Device fabrication:

The photosensitive resin was used to fabricate the fabricate the microchip mold through 3D laser printing technology. The concrete process can be divided to five steps. First, the linear arrays of bottom microcavities were formed from the mixture of the Sylgard 184 silicone elastomer base and curing agent at a ratio of 10:1 (W/W). To prevent the deformation of the 3D printing mold, the curing temperature was 60 °C for 3h. Second, a 1H, 1H, 2H, 2H-perfluorooctyltrichlorosilane layer was deposited on top of the cured photosensitive resin under a vacuum to provide mechanical resistance for the second molding. Third, a reusable biopsy punch was used to punch holes in both ends of the chip for inlet and outlet. Fourth, a 40 mm × 50 mm × 0.15 mm (width × length × thickness) glass slide was bound on the final molding microstructure with oxygen plasma for 20s and keep at 90°C for 10 min. Fifth, a modified lead zirconate titanate transducer (Pz26, Ferroperm Co., Denmark) was glued (III) to the glass slide.

B. Simulation Methods:

The simulation results of acoustic microflow are obtained by finite element analysis software COMSOL Multiphysics. Based on acoustic streaming theory and some necessary assumptions for simplifications, the standard perturbation theory to first order in the amplitude of the oscillating (MHz ultrasound) boundary conditions. Then we got the numerical results of acoustic streaming distribution.

C. Animal experiments:

Five-week-old female BALB/c mice (15 ± 1.1 g) were purchased from Laboratory Animal Center, Academy of Military Medical Science of People's Liberation Army (Beijing, China). Mice were allowed to acclimatize, without handling, for a minimum of 1 week before the start of experiments. All animal experiments were conducted using protocols approved by the Institutional Animal Care and Use Committee at the Institute of Tumors of the Chinese Academy of Medical Sciences.

D. Blood sample preparation:

Mice were randomly divided into 2 groups. Sham operated control and malignant tumors group. Control group: PBS were injected into the right-side axillary mammary gland; Tumors group: mice was euthanized while 1×10^5 4T1 cells stably expressing the firefly luciferase gene (4T1-Luc) were injected into the right-side axillary mammary gland of the 8 mice[25]. After implantation, the tumor volumes were measured every 5 days by in vivo image. On day 20 after implantation, surgical excision of the primary tumors was performed under sterile conditions. Blood (50μl) was taken from the eye socket at the same day after the operation. The blood was allowed to sit at room temperature for 20 minutes, then centrifuged at 4,000 r/min for 15 minutes. The precipitation was fixed with 4% paraformaldehyde (PFA) at room temperature for 20 minutes, then centrifuged at 6500 r/min for 15 minutes. Dilute the precipitation in a ratio of 1 to 4 with a PBS buffer.

E. CTCs capture from whole blood sample

During the capture experiment, the acoustic device was fixed on the stage of an upright fluorescence microscope (BX51WI, Olympus, Japan). An individual syringe pumps (neMESYS, cetoni GmbH, Germany) was used to control the sample fluid flows. Before starting the injection, first remove the bubbles in the channel with ethanol, then rinse with a phosphoric acid buffer for 5 minutes. The sample fluid was then injected to the device at a flow rate of 10 μL/s. The acoustic wave was excited by applying a radio frequency (RF) signal to the IDTs on the piezoelectric substrate. The RF signal was generated by a function generator (E4422B; Agilent, USA) and an amplifier (25A100A; Amplifier Research, USA). The frequency was set at 19.9 MHz, and the power inputs ranged from 32 to 35 dBm. The videos and images of sample fluid were got from a high-speed camera.

F. Bioluminescence imaging:

IVIS Lumina small-animal imaging system were used to measure the distribution of 4T1-Luc in animal model. The bioluminescence imaging was performed after the implanted of 4T1-Luc for 10 and 20 days to detect the growth of tumor in situ. After the surgical excision, the bioluminescence imaging was performed to measure the surgery effect. Then Imaging is done every 5 days until a metastatic is formed. The tissue of animal model was image to test the cancer cell distribution in different tissue.

III. RESULTS AND DISCUSSION

A. The acoustic microfluidic device design:

The acoustic microfluidic device consists of a polydimethylsiloxane (PDMS) microfluidic channel, a glass slide and a piezoelectric transducer (Fig. 1a). In the PDMS channel, linear arrays of bottom microcavities with a diameter of 100μm and height of 80μm were designed. 1000 microcavities were equally distributed in the PDMS channel in a 100 × 10 array over the operating area. The glassed slide with a thickness of 150μm were bond on the PDMS layer, which can transport acoustic energy from transducer to liquid in the PDMS Acoustic energy. The piezoelectric transducer is connected to the glassed slide to produce sound waves at a specific frequency and voltage that react with the liquid in the microchannel to produce a microflow field at the position of the microcavities (Fig. 1b).

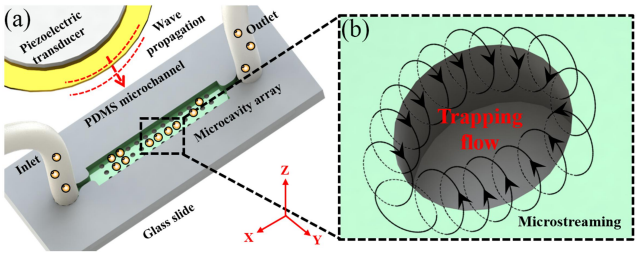

Fig.1: The acoustic microfluidic device design. a) Components of acoustic microfluidic include a PDMS microchannel with bottom microcavity array where can form trapping flow, a piezoelectric transducer to produce acoustic wave and a glass slide was used to transport acoustic energy; b) Microstreaming flows (trapping flow) formed in fluid as a steady flow driven by the absorption of high-amplitude acoustic vibration are utilized to achieve.

B. The generation of acoustic microstreaming through simulation analysis:

The disturbance of the liquid in the microchannel caused by the sound wave generated by the piezoelectric transducer was simulated and analyzed by COMSOL Multiphysics. In theory, particles in microflow channels are subjected to two forces simultaneously, the acoustic radiation force (ARF) arising from sound waves scattering on the particles (F^{rad}), and the Stokes drag force generated by the induced acoustic streaming flow (F^{drag}). As shown in figure 2, two microvortexs were formed from two acoustic force. Based on the standard perturbation theory to sound boundary conditions, F^{rad} and F^{drag} are depend on the diameter of particles. When the size of particles is less than 2.5 μm, such as cell, F^{drag} is the the main force. As a result, the capture fore is from the surface microvotexs corresponding to F^{drag} which can be calculated by the following formula:

$$F^{drag} = 6\pi\eta a(< v_2 > - u) \quad (1)$$

where η is the dynamic viscosity, u is the time-averaged velocity of acoustic microstreaming and a is the diameter of particles. Therefore, the diameter difference can be applicated to separate the target particles from a mixture, such as the capture CTCs from the patient blood.

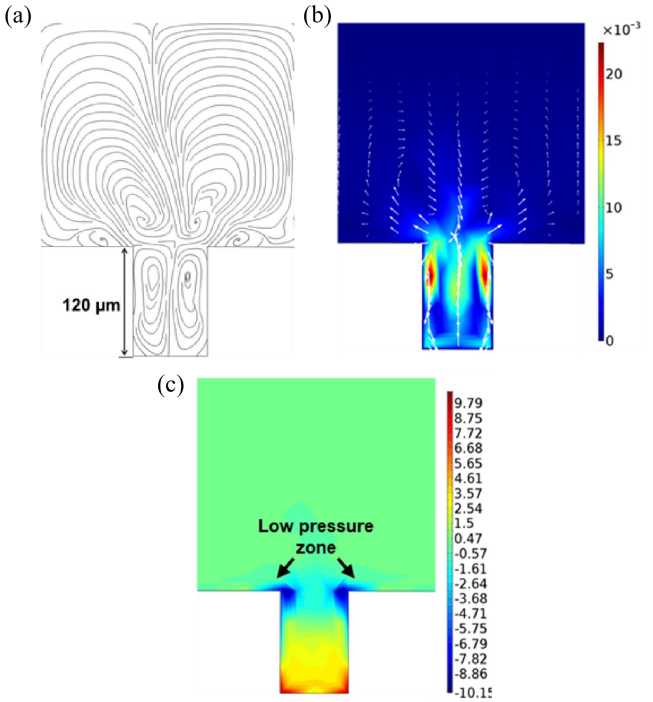

Fig.2: Simulation results of vibration-induced acoustic streaming. a) Finite element method (FEM) simulation illustrating the calculated streamline of the flow field b) FEM simulation illustrating the acoustic microstreaming generated by vibrating bottom microcavity, and the results of the velocity vector field (unit: m/s). c) Plot of the pressure field in X-Z plane (Pa).

C. Circulating tumor cell separation from the blood sample:

To evaluate the capture capacity for CTC of the acoustofluidic device, which can be used to predict the possibility of metastasis recurrence after tumor resection, we implanted murine BALB/c-derived 4T1 cells stably expressing the firefly luciferase gene (4T1-Luc) into the mammary fat pad of mice. The experimental design, including the timeline of establishment of tumor allografts, tumor excision, whole blood sample obtained and detection of tumor metastasis, is shown in Fig. 3a. The pretreatment for the whole blood sample were shown in Fig. 3b. To keep the stiffness of the cell, we fixed the cell, including red blood cells (RBC), white blood cells (WBC), CTC, with 4% paraformaldehyde (PFA). The treated blood samples were injected to the device at the speed of 10μL, and turn on the ultrasonic generator to get the vibrating bottom microcavity at 4.3 kHz and 20 Vp–p. When the blood sample go through the operating area with microcavity array, the vibration-induced streaming flows allowed capturing nearby flowing cancer cells. The rest of the RBCs and WBCs continue their movement downstream toward the outlet region (Fig. 3c).

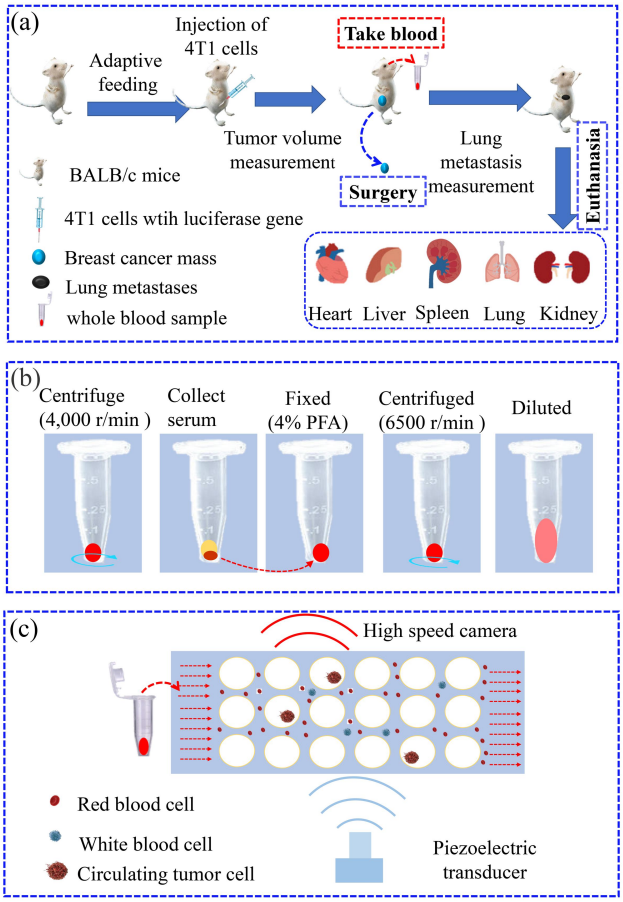

Fig. 3: The schematic diagram of the CTC capture experiment. (a) The experiment design for the evaluation after tumor resection; (b) The pretreatment of the whole blood sample; (c) The capture process of the acoustofluidic device for CTC.

We surgically removed the primary tumors 20 days after implantation of 4T1-Luc cells to get the whole blood sample, which used to measure the possibility of tumor metastasis after surgical treatment. As shown in Fig. 4(a), the breast tumor has already formed at the third pair of breast fat pads and we removed the tumor surgically, showing that there was no residual cancer cell in the primary site or metastasis at other tissue (Fig.4b). This indicate that we treated the mice by surgery before the formation of metastasis. After the surgery, the whole blood samples were got from orbital and threated the sample as shown in Fig. 3b. The number of CTCs were captured by the acoustofluidic device was shown in the representative image (Fig.4c). The captured CTCs in model A is more than the model B. The previously research has demonstrated that the more CTC in blood, the more likely they are to metastasize. It is reasonable to predicate that the model A will metastasize. As predicated, the metastasize firstly formed at the first pair of breasts after 10 days after the surgery (Fig.4d). What is more, at the 15th day, the metastasis can be observed at lung for model A. Model B, however, did not form the metastasis until the end of the experiment (Fig.4e). At day 16, mice were euthanized to verify enhanced lung metastases due to the more CTC existent in blood. As shown in Fig. 4f, the fluorescence signal in lung of model A is obviously stronger than the model B, which indicate that the metastasis formation of breast cancer cell at lung because of the more CTC in blood. The metastasize data support that the acoustofluidic device design in this study has capability to capture the CTC from the small amount of whole blood sample, and to predicate the potential of metastatic successfully.

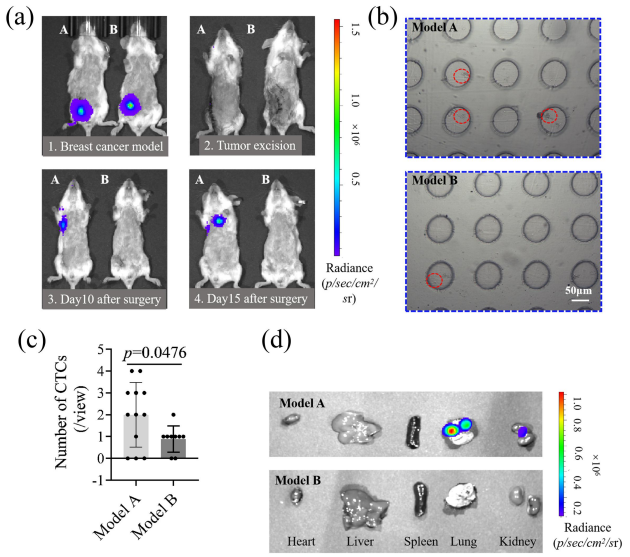

Fig.4: Evaluation of lung metastases of tumors based on the capture capability of acoustofluidic device for CTC. (a) The breast cancer tumor formation after implant 4T1-Luc 20 days at the third pair of breast fat pads, treated mice after surgery, metastatic lung lesion formation was monitored by bioluminescence imaging at days 10 and 15 after tumor removal; (b) The acoustofluidic device capture the CTCs; (c) Statistic analysis for the number of CTCs captured by the acoustofluidic device; (d) Lung metastastic lesions were assessed by bioluminescence imaging upon euthanasia.

IV. Conclusion

In this study, a novel acoustofluidic device were successful used to separate the CTCs from the whole blood sample. As far as information is available, this is the first systematic evaluation of the function of CTCs isolation in tumor metastasis under conditions that completely simulated the tumor treatment procedure in clinically. When the vibrating bottom cavity array receives ultrasonic waves from the ultrasonic generator, the steady localized microstreaming forces were produced to capture the CTCs. The CTC is the "true" CTCs from the blood of cancer "patients" after surgery, not the simulated CTCs. We predicted the likelihood of metastasis based on the number of CTCs captured. In addition, further observation of tumor metastasis supported our hypothesis. In conclusion, the novel acoustofluidic device can efficiently capture CTCs and predict the likelihood of metastasis in " patients" after surgery. This can provide powerful support to clinicians in formulating treatment plans for patients with cancer after surgery.

REFERENCES

[1] J. Massagué, and A. C. Obenauf, "Metastatic colonization by circulating tumour cells," *Nature,* vol. 529, no. 7586, pp. 298-306, 2016/01/01, 2016.

[2] M. Brown, F. P. Assen, A. Leithner, J. Abe, H. Schachner, G. Asfour, Z. Bago-Horvath, J. V. Stein, P. Uhrin, M. Sixt, and D. Kerjaschki, "Lymph node blood vessels provide exit routes for metastatic tumor cell dissemination in mice," *Science,* vol. 359, no. 6382, pp. 1408-1411, 2018.

[3] K. Naxerova, J. G. Reiter, E. Brachtel, J. K. Lennerz, M. van de Wetering, A. Rowan, T. Cai, H. Clevers, C. Swanton, M. A. Nowak, S. J. Elledge, and R. K. Jain, "Origins of lymphatic and distant metastases in human colorectal cancer," *Science,* vol. 357, no. 6346, pp. 55-60, 2017.

[4] E. Rossi, and F. Fabbri, "CTCs 2020: Great Expectations or Unreasonable Dreams," *Cells,* vol. 8, no. 9, pp. 989, 2019.

[5] B. Weigelt, J. L. Peterse, and L. J. van't Veer, "Breast cancer metastasis: markers and models," *Nature Reviews Cancer,* vol. 5, no. 8, pp. 591-602, 2005/08/01, 2005.

[6] S. Gupta, J. Li, G. Kemeny, R. L. Bitting, J. Beaver, J. A. Somarelli, K. E. Ware, S. Gregory, and A. J. Armstrong, "Whole Genomic Copy Number Alterations in Circulating Tumor Cells from Men with Abiraterone or Enzalutamide-Resistant Metastatic Castration-Resistant Prostate Cancer," *Clinical Cancer Research,* vol. 23, no. 5, pp. 1346-1357, 2017.

[7] D. C. Danila, G. Heller, G. A. Gignac, R. Gonzalez-Espinoza, A. Anand, E. Tanaka, H. Lilja, L. Schwartz, S. Larson, M. Fleisher, and H. I. Scher, "Circulating Tumor Cell Number and Prognosis in Progressive Castration-Resistant Prostate Cancer," *Clinical Cancer Research,* vol. 13, no. 23, pp. 7053-7058, 2007.

[8] F. Tanaka, K. Yoneda, N. Kondo, M. Hashimoto, T. Takuwa, S. Matsumoto, Y. Okumura, S. Rahman, N. Tsubota, T. Tsujimura, K. Kuribayashi, K. Fukuoka, T. Nakano, and S. Hasegawa, "Circulating Tumor Cell as a Diagnostic Marker in Primary Lung Cancer," *Clinical Cancer Research,* vol. 15, no. 22, pp. 6980-6986, 2009.

[9] A. Lucci, C. Hall, S. P. Patel, B. Narendran, J. B. Bauldry, R. Royal, M. Karhade, J. R. Upshaw, J. A. Wargo, I. C. Glitza, M. K. K. Wong, R. N. Amaria, H. A. Tawbi, A. Diab, M. A. Davies, J. E. Gershenwald, J. E. Lee, P. Hwu, and M. I. Ross, "Circulating tumor cells and early relapse in node-positive melanoma," *Clinical Cancer Research*, pp. clincanres.2670.2019, 2020.

[10] W. J. Allard, J. Matera, M. C. Miller, M. Repollet, M. C. Connelly, C. Rao, A. G. J. Tibbe, J. W. Uhr, and L. W. M. M. Terstappen, "Tumor Cells Circulate in the Peripheral Blood of All Major Carcinomas but not in Healthy Subjects or Patients With Nonmalignant Diseases," *Clinical Cancer Research,* vol. 10, no. 20, pp. 6897-6904, 2004.

[11] J. M. Jackson, M. A. Witek, J. W. Kamande, and S. A. Soper, "Materials and microfluidics: enabling the efficient isolation and analysis of circulating tumour cells," *Chemical Society Reviews,* vol. 46, no. 14, pp. 4245-4280, 2017.

[12] A. M. C. Barradas, and L. W. M. M. Terstappen, "Towards the Biological Understanding of CTC: Capture Technologies, Definitions and Potential to Create Metastasis," *Cancers,* vol. 5, no. 4, pp. 1619-1642, 2013.

[13] P. Li, Z. S. Stratton, M. Dao, J. Ritz, and T. J. Huang, "Probing circulating tumor cells in microfluidics," *Lab Chip,* vol. 13, no. 4, pp. 602-9, Feb 21, 2013.

[14] S. Nagrath, L. V. Sequist, S. Maheswaran, D. W. Bell, D. Irimia, L. Ulkus, M. R. Smith, E. L. Kwak, S. Digumarthy, A. Muzikansky, P. Ryan, U. J. Balis, R. G. Tompkins, D. A. Haber, and M. Toner, "Isolation of rare circulating tumour cells in cancer patients by microchip technology," *Nature,* vol. 450, no. 7173, pp. 1235-1239, 2007/12/01, 2007.

[15] O. Vermesh, A. Aalipour, T. J. Ge, Y. Saenz, Y. Guo, I. S. Alam, S.-m. Park, C. N. Adelson, Y. Mitsutake, J. Vilches-Moure, E. Godoy, M. H. Bachmann, C. C. Ooi, J. K. Lyons, K. Mueller, H. Arami, A. Green, E. I. Solomon, S. X. Wang, and S. S. Gambhir, "An intravascular magnetic wire for the high-throughput retrieval of circulating tumour cells in vivo," *Nature Biomedical Engineering,* vol. 2, no. 9, pp. 696-705, 2018/09/01, 2018.

[16] C. L. Sawyers, "The cancer biomarker problem," *Nature,* vol. 452, no. 7187, pp. 548-552, 2008/04/01, 2008.

[17] G. Morstyn, J. Brown, U. Novak, J. Gardner, J. Bishop, and M. Garson, "Heterogeneous Cytogenetic Abnormalities in Small Cell Lung Cancer Cell Lines," *Cancer Research,* vol. 47, no. 12, pp. 3322-3327, 1987.

[18] E. Sueoka, N. Sueoka, Y. Goto, S. Matsuyama, H. Nishimura, M. Sato, S. Fujimura, H. Chiba, and H. Fujiki, "Heterogeneous Nuclear Ribonucleoprotein B1 as Early Cancer Biomarker for Occult Cancer of Human Lungs and Bronchial Dysplasia," *Cancer Research,* vol. 61, no. 5, pp. 1896-1902, 2001.

[19] P. Li, Z. Mao, Z. Peng, L. Zhou, Y. Chen, P.-H. Huang, C. I. Truica, J. J. Drabick, W. S. El-Deiry, M. Dao, S. Suresh, and T. J. Huang, "Acoustic separation of circulating tumor cells," *Proceedings of the National Academy of Sciences,* vol. 112, no. 16, pp. 4970-4975, 2015.

[20] P. Bankó, S. Y. Lee, V. Nagygyörgy, M. Zrínyi, C. H. Chae, D. H. Cho, and A. Telekes, "Technologies for circulating tumor cell separation from whole blood," *Journal of Hematology & Oncology,* vol. 12, no. 1, pp. 48, 2019/05/14, 2019.

[21] R. Gao, L. Cheng, S. Wang, X. Bi, X. Wang, R. Wang, X. Chen, Z. Zha, F. Wang, X. Xu, G. Zhao, and L. Yu, "Efficient separation of tumor cells from

untreated whole blood using a novel multistage hydrodynamic focusing microfluidics," *Talanta,* vol. 207, pp. 120261, 2020/01/15/, 2020.

[22] M. E. Warkiani, B. L. Khoo, L. Wu, A. K. P. Tay, A. A. S. Bhagat, J. Han, and C. T. Lim, "Ultra-fast, label-free isolation of circulating tumor cells from blood using spiral microfluidics," *Nature Protocols,* vol. 11, no. 1, pp. 134-148, 2016/01/01, 2016.

[23] M. Antfolk, S. H. Kim, S. Koizumi, T. Fujii, and T. Laurell, "Label-free single-cell separation and imaging of cancer cells using an integrated microfluidic system," *Scientific Reports,* vol. 7, no. 1, pp. 46507, 2017/04/20, 2017.

[24] M. Wu, P.-H. Huang, R. Zhang, Z. Mao, C. Chen, G. Kemeny, P. Li, A. V. Lee, R. Gyanchandani, A. J. Armstrong, M. Dao, S. Suresh, and T. J. Huang, "Circulating Tumor Cell Phenotyping via High-Throughput Acoustic Separation," *Small,* vol. 14, no. 32, pp. 1801131, 2018.

[25] X. Lu, Y. Zhu, R. Bai, Z. Wu, W. Qian, L. Yang, R. Cai, H. Yan, T. Li, V. Pandey, Y. Liu, P. E. Lobie, C. Chen, and T. Zhu, "Long-term pulmonary exposure to multi-walled carbon nanotubes promotes breast cancer metastatic cascades," *Nature Nanotechnology,* vol. 14, no. 7, pp. 719-727, 2019/07/01, 2019.